Photochemical Ring-Opening Reactions Are Complete in Picoseconds: A Time-Resolved UV Resonance Raman Study of 1,3-Cyclohexadiene

Philip J. Reid,[1a] Stephen J. Doig,[1b] Steven D. Wickham, and Richard A. Mathies*

Contribution from the Department of Chemistry, University of California, Berkeley, California 94720

Received November 11, 1992

Abstract: Photoproduct formation, vibrational, and conformational relaxation kinetics in the photochemical ring-openings of 1,3-cyclohexadiene (CHD) and α-phellandrene (α-PHE) are determined by picosecond, time-resolved UV Stokes and anti-Stokes resonance Raman spectroscopy. The frequency-doubled output from an amplified, synchronously pumped dye laser system was used to perform transient, two-color resonance Raman Stokes experiments on the photoconversion of CHD to *cis*-hexatriene (c-HT) and of α-PHE to 3,7-dimethyl-1,3,5-octatriene (OT). The appearance time of the Stokes scattering from ground-state c-HT is 6 ± 1 ps, while that of OT is 11 ± 2 ps. In both reactions, the photoproduct anti-Stokes ethylenic intensity appears with a time constant of 8 ± 2 ps and decays in 9 ± 2 ps. This similarity demonstrates that the photoproduct appearance and intermolecular vibrational relaxation kinetics are not dramatically affected by the presence of alkyl substituents. Analysis of the photoproduct spectral evolution in the Stokes and anti-Stokes data as well as the observation of Raman lines characteristic of the *all-cis* conformer in the anti-Stokes data demonstrates that *all-cis*-HT first appears on the ground-state surface and then undergoes conformational relaxation to produce *mono-s-cis*-HT with a time constant of 7 ps. The photoproduct anti-Stokes ethylenic and single-bond stretch intensities further demonstrate that the initial photoproduct temperature at 4 ps is 1500 ± 500 K and that the cooling time is 15 ps. This is the first complete analysis of the photoproduct formation, vibrational, and conformational relaxation dynamics characteristic of photochemical pericyclic ring-opening reactions.

Introduction

Photoexcitation of 1,3-cyclohexadiene (CHD) in the condensed phase initiates an efficient (ϕ = 0.4) electrocyclic ring-opening reaction.[2-7] The stereochemistry of the *cis*-hexatriene (c-HT) photoproduct (and its substituted analogs) is consistent with a conrotatory ring-opening, in agreement with predictions based on the conservation of orbital symmetry in pericyclic rearrangements.[8-11] Although electrocyclic ring-opening reactions are central to our understanding of polyene and vitamin D photochemistry,[12-14] the excited-state dynamics and overall kinetics of these reactions have only recently been explored. Resonance Raman intensity analysis has demonstrated that the initial excited-state evolution of CHD is along the conrotatory reaction coordinate and that depopulation of this state occurs in ~10 femtoseconds.[15,16] Picosecond time-resolved UV resonance Raman spectroscopy has shown that the c-HT photoproduct appears on the ground-state surface ~8 ps after photolysis.[17] Similar photoproduct production kinetics were observed in the electrocyclic ring-openings of α-phellandrene, 1,3,5-cyclooctatriene, and 7-dehydrocholesterol, demonstrating that picosecond formation times are a general feature of electrocyclic ring-opening reactions.[18,19] Recent experiments have also shown that the photochemical hydrogen migration in 1,3,5-cycloheptatriene (CHT) is complete in only 26 ps.[20] Furthermore, Raman scattering from vibrationally unrelaxed CHT was observed, suggesting that ground-state vibrational and structural relaxation are important in the dynamics of photochemical rearrangements.

In this paper, we present a complete analysis of the picosecond time-resolved Stokes and anti-Stokes resonance Raman spectra of CHD and α-phellandrene (α-PHE, an alkyl-substituted CHD) which characterizes the conformational and vibrational relaxation kinetics of the photoproducts (Scheme I).[2,21-23] The photoproduct appearance time and the rate of vibrational relaxation of CHD and α-PHE are found to be similar, demonstrating that the dynamics of photoproduct formation are not altered by the

* Author to whom correspondence should be addressed.
(1) Present Address: (a) Department of Chemistry, University of Minnesota, Minneapolis MN 55455. (b) The Mayo Clinic, Rochester, MN 55905.

(2) de Kock, R. J.; Minnaard, N. G.; Havinga, E. *Rec. Trav. Chim. Pays-Bas* **1960**, *79*, 922–934.
(3) Crowley, K. J. *J. Org. Chem.* **1968**, *33*, 3679–3686.
(4) Dauben, W. G.; Rabinowitz, J.; Vietmeyer, N. D.; Wendschuh, P. H. *J. Am. Chem. Soc.* **1972**, *94*, 4285–4292.
(5) Dauben, W. G.; Kellogg, M. S.; Seeman, J. I.; Vietmeyer, N. D.; Wendschuh, P. H. *Pure Appl. Chem.* **1973**, *33*, 197–215.
(6) Dauben, W. G.; McInnis, E. L.; Michno, D. M. *Rearrangements in Ground and Excited States*; Academic Press: New York, 1980; Vol. 3, pp 91–129.
(7) Jacobs, H. J. C.; Havinga, E. *Adv. Photochem.* **1979**, *11*, 305–373.
(8) Hoffmann, R.; Woodward, R. B. *Acc. Chem. Res.* **1968**, *1*, 17–22.
(9) Fukui, K. *Acc. Chem. Res.* **1971**, *4*, 57–64.
(10) Woodward, R. B.; Hoffmann, R. *The Conservation of Orbital Symmetry*, 1st ed.; Verlag Chemie International: Weinheim/Deerfield Beach, 1970.
(11) Longuet-Higgins, H. C.; Abrahamson, E. W. *J. Am. Chem. Soc.* **1965**, *87*, 2045–2046.
(12) Hudson, B. S.; Kohler, B. E.; Schulten, K. In *Excited States*; Lim, E. C., Ed.; Academic Press: New York, 1982; Vol. 6, pp 1–95.
(13) Havinga, E.; de Kock, J. J.; Rappoldt, M. P. *Tetrahedron* **1960**, *11*, 276–284.
(14) Rappoldt, M. P.; Havinga, E. *Recl. Trav. Chim. Pays-Bas* **1960**, *79*, 369–381.
(15) Trulson, M. O.; Dollinger, G. D.; Mathies, R. A. *J. Am. Chem. Soc.* **1987**, *109*, 586–587.
(16) Trulson, M. O.; Dollinger, G. D.; Mathies, R. A. *J. Chem. Phys.* **1989**, *90*, 4274–4281.
(17) Reid, P. J.; Doig, S. J.; Mathies, R. A. *Chem. Phys. Lett.* **1989**, *156*, 163–168.
(18) Reid, P. J.; Doig, S. J.; Mathies, R. A. *J. Phys. Chem.* **1990**, *94*, 8396–8399.
(19) Gottfried, N.; Kaiser, W.; Braun, M.; Fuss, W.; Kompa, K. L. *Chem. Phys. Lett.* **1984**, *110*, 335–339.
(20) Reid, P. J.; Wickham, S. D.; Mathies, R. A. *J. Phys. Chem.* **1992**, *96*, 5720–5724.
(21) Baldwin, J. E.; Krueger, S. M. *J. Am. Chem. Soc.* **1969**, *91*, 6444–6447.
(22) Crowley, K. J.; Erickson, K. L.; Eckell, A.; Meinwald, J. *J. Chem. Soc., Perkin Trans. 1* **1973**, 2671–2679.
(23) Spangler, C. W.; Hennis, R. P. *J. Chem. Soc., Chem. Commun.* **1972**, 24–25.

0002-7863/93/1515-4754$04.00/0

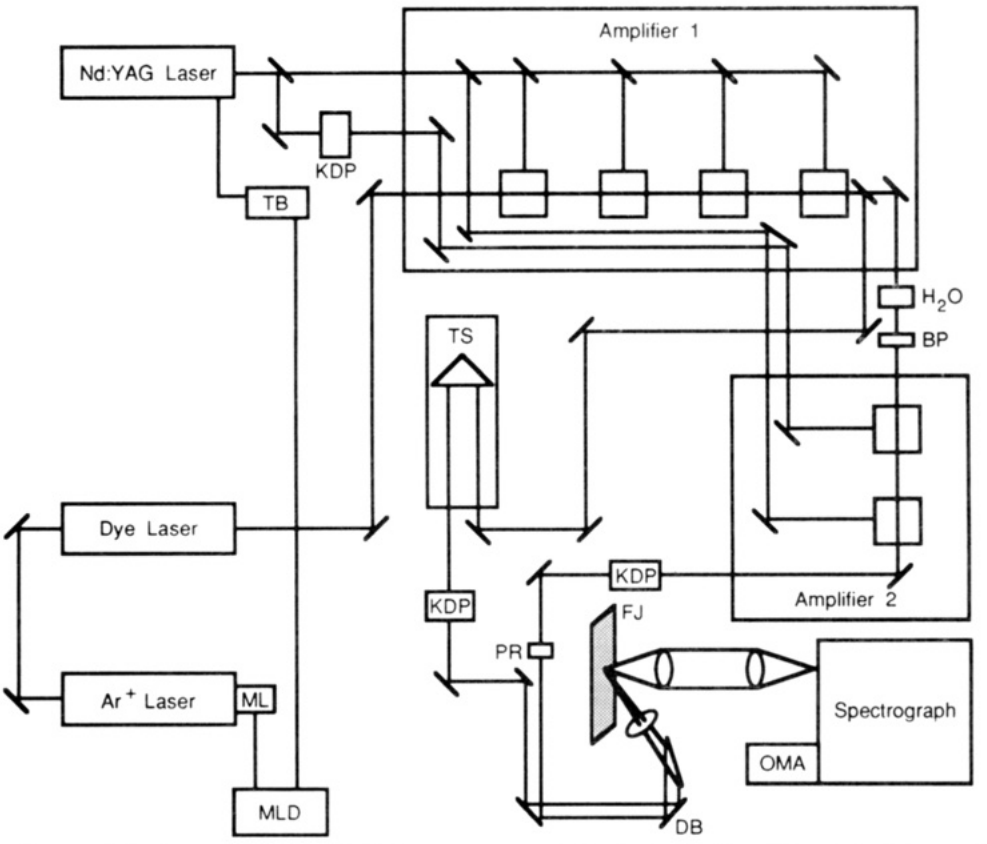

Figure 1. Schematic diagram of the picosecond two-color UV Raman apparatus. BP = band-pass filter, DB = dichroic beam splitter, FJ = flowing jet, H_2O = water continuum cell, KDP = potassium dihydrogen phosphate doubling crystal, ML = mode locker, MLD = mode locker driver, OMA = optical multichannel analyzer, PR = polarization rotator, TB = timing box, TS = translation stage.

Scheme I

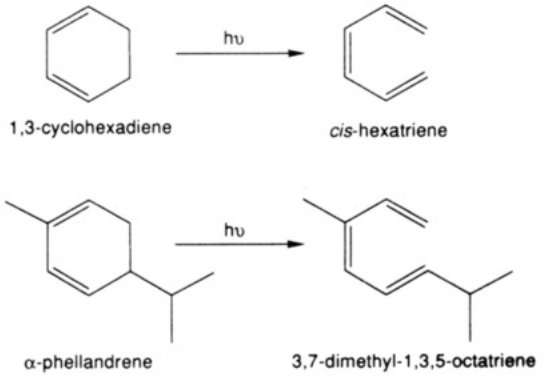

presence of alkyl substituents. Furthermore, the evolution of the photoproduct ethylenic and single-bond anti-Stokes intensities demonstrate that the initial temperature of c-HT is significantly elevated (1500 ± 500 K), with cooling to ambient temperature occurring in 15 ps. Finally, the spectral evolution in the time-resolved Stokes and anti-Stokes spectra provides a direct observation of the *di-s-cis*-HT photoproduct on the ground-state surface as well as its subsequent conformational isomerization to *mono-s-cis*-HT. These results provide the first complete picture of photoproduct formation and vibrational relaxation dynamics in photochemical electrocyclic ring-opening reactions.

Experimental Section

Resonance Raman Spectroscopy. The picosecond UV Raman apparatus is presented in Figure 1. The 568-nm output of a dye laser synchronously pumped by a mode-locked Ar^+ ion laser was delivered to a four-stage amplifier which has been described in detail earlier.[24] Fluorescein 548 in basic ethanol was placed in the first stage of the amplifier, while Rhodamine 6G was used in the remaining cells. The amplifier was pumped by 140 mJ from an amplified Nd:YAG laser (Continuum YG581-C) operated at 50 Hz, resulting in amplifier output energies of 1.2 mJ/pulse with a background-free autocorrelation FWHM (full width at half maximum) of 2.0 ps and amplified spontaneous emission (ASE) of 1.5%.

For the two-color Stokes experiment, the amplifier output was split into two beams with 25% of the power delivered to an optical delay line and frequency doubled with a 2-mm piece of KDP. The residual fundamental was removed from the doubled light by a dichroic beamsplitter, and the resulting beam at 284 nm served as the probe. The actinic pulse was generated by focusing the remaining output of the amplifier into a 7-cm-long cell of D_2O for continuum generation. A 2-nm-wide bandpass filter (Omega Optics) centered at 550 nm was used to select the frequency of interest from the white-light continuum, and this beam was directed to a two-stage amplifier pumped by the same Nd:YAG laser used for the first amplifier. Fluorescein 548 in basic ethanol was used in both stages, resulting in typical pulse energies of 600 μJ with 5% ASE and an autocorrelation FWHM of 2.0 ps. The 550-nm beam was frequency doubled with a 1-mm piece of KDP, and the resulting light at 275 nm served as the actinic pulse. Cross-correlation of the 284-nm probe and 275-nm pump beams was accomplished by the two-photon-dependent ionization of DABCO (1,4-diazabicyclo[2.2.2]octane (Aldrich)), resulting in a cross-correlation FWHM of 1.8 ps. The details of this procedure have been described elsewhere.[20,25] This technique also served to establish zero time delay between the pump and probe beams.

For the one-color anti-Stokes experiments, 25% of the amplifier output was used to generate the probe (see above), while the remainder of the amplified beam was frequently doubled with a 1-mm piece of KDP with the 284-nm light serving as the actinic pulse. Cross-correlation of the pump and probe beams was also accomplished by the two-photon-dependent ionization of DABCO, resulting in a FWHM of 1.7 ps.

Detailed experimental conditions for the Stokes and anti-Stokes experiments were as follows. Solutions of 75 mM 1,3-cyclohexadiene (Aldrich, 98%) or (*R*)-(α)-phellandrene (Fluka, 99%) in HPLC grade cyclohexane (Fisher) were employed. Concentrations from 30 to 200 mM were studied, and no change in kinetics was observed. In all

(24) Doig, S. J.; Reid, P. J.; Mathies, R. A. *J. Phys. Chem.* **1991**, *95*, 6372–6379.

(25) Szatmari, S.; Racz, B.; Schaffer, F. P. *Opt. Commun.* **1987**, *62*, 271–276.

experiments, a 250-mL sample reservoir was maintained at 10 °C by immersion in an ice bath, and the change in concentration over the course of the experiment was kept to <5%. The pump and probe beams were focused onto a flowing jet of the sample utilizing a backscattering geometry. The flow rate of the jet was sufficient to replenish the illuminated volume between successive sets of pulses. For the anti-Stokes experiments, pulse energies of 16 μJ in the pump and 3.6 μJ in the probe were focused onto the jet with a 100-mm focal length spherical lens to an area of 3×10^{-4} cm^2. For the Stokes experiment, pulse energies of 12.5 μJ in the pump and 3.6 μJ in the probe were employed. The polarization of the pump was rotated to 55° relative to that of the probe to minimize the contribution of molecular rotations to the observed kinetics. The intensity of the product lines responded linearly with a 5-fold reduction in pump power. The photoproduct formation kinetics under conditions identical to the anti-Stokes experiment were determined and found to be equivalent to those of the two-color Stokes experiment.

Raman scattering was collected with standard UV grade refractive optics and delivered to a Spex 500M, f/4 spectrograph equipped with a 1200 g/mm classically ruled grating (blaze = 500 nm) operated in second order. An entrance slit width of 200-μm for the anti-Stokes experiments and 150 μm for the Stokes data resulted in 20- and 15-cm^{-1} resolution, respectively. The scattering was detected with a PAR Model 1421 intensified diode array. In the anti-Stokes experiment, the detector was gated by applying a 400 ns, 200 V pulse to the detector intensifier (PAR Model 1304) synchronous with the firing of the Nd:YAG Q-switch. Vibrational frequencies are accurate to ±4 cm^{-1} in the anti-Stokes spectra and ±2 cm^{-1} in the Stokes spectra.

The Raman spectra at a given time delay were collected by interleaving integrations with the "probe-only", the "pump-only", and the "pump-and-probe" incident on the sample. Fifteen integrations of 20 s and 12 integrations of 120 s were summed at each time delay for the Stokes and anti-Stokes spectra, respectively. The pump-only spectrum was directly subtracted from the pump-and-probe spectrum, resulting in the "probe-with-photolysis" spectrum. From this spectrum the probe-only was directly subtracted, resulting in the difference data reported here. In the Stokes experiment, correction for the change in the optical absorption of the sample at each time point was accomplished by normalizing the data to changes in the 801-cm^{-1} solvent line. In the experiments on CHD, this correction was 12% at early times and was ±5% for delays between 10 and 100 ps. For the experiments of α-PHE, this correction was ±2% at all delay times.

Computational Methods

Normal mode calculations on the single-bond isomers of c-HT were performed using the QCFF-π method.[26] The geometry of each c-HT isomer (*all-cis*, *mono-s-cis*, and *di-s-trans*) was minimized, and the vibrational spectrum was then calculated. Resonance Raman intensities were predicted by determining the excited-state slope in the Franck–Condon region along each normal coordinate. Only those modes predicted to demonstrate significant Raman intensity are reported here. The resonance Raman anti-Stokes cross sections for CHD and c-HT were calculated utilizing a sum-over-states calculation which specifically included thermal excitation in vibrational levels whose Boltzmann population is ≥0.001 for all Raman active modes.[27] Mode displacements, E_{00} energies, and homogeneous and inhomogeneous broadening parameters were obtained from previous resonance Raman intensity analyses.[16,28,29]

Results

1,3-Cyclohexadiene Raman Kinetics. Stokes Resonance Raman Spectra. Two-color Stokes Raman spectra of the 1,3-cyclohexadiene (CHD) to *cis*-hexatriene (c-HT) photoconversion are presented in Figure 2. In the 0-ps spectrum, negative intensity at 1578 and 1323 cm^{-1} is observed and assigned to the ground-state depletion of CHD created by the pump pulse. The negative cyclohexane lines at 801, 1027, 1155, 1267, and 1445 cm^{-1} indicate that at this delay time, the optical absorbance of the sample has also increased due the presence of the actinic pulse. After correction for this optical absorbance change, the remaining negative CHD intensity at 1578 cm^{-1} indicates that the extent of photolysis is 6%. In the 4-ps spectrum, the positive intensity at 390, 1236, and 1610 cm^{-1} is assigned as scattering from the c-HT photoproduct. Partial recovery of the CHD depletion is also observed, consistent with ground-state recovery and a decrease in the optical absorbance of the sample. The intensity of the c-HT lines increases between 8 and 22 ps, by which time an additional photoproduct feature at 1318 cm^{-1} is also apparent. At this time, the lines due to the ethylenic and single-bond stretch of c-HT have shifted from 1610 to 1625 cm^{-1} and from 1236 to 1249 cm^{-1}, respectively. By 100 ps, the spectrum of the photoproduct exhibits a second ethylenic line at 1572 cm^{-1}. The slight positive intensity of the cyclohexane line at 801 cm^{-1} indicates that the optical absorbance of the sample has decreased relative to the probe-only spectrum. Although positive intensity at 1572 cm^{-1} could be consistent with scattering from CHD, the 0.4 photochemical quantum yield should result in negative CHD intensity even after consideration of the decrease in sample optical absorbance. Therefore, the positive intensity at 1572 cm^{-1} must be due to the presence of c-HT. No further evolution in the spectrum is observed for delays between 100 ps and 1 ns. As an initial measurement of the production kinetics, the photoproduct ethylenic intensity was fit to a single exponential (not shown), with best fit to a single exponential resulting in an appearance time of 7 ± 1.5 ps in agreement with our previous results.[17]

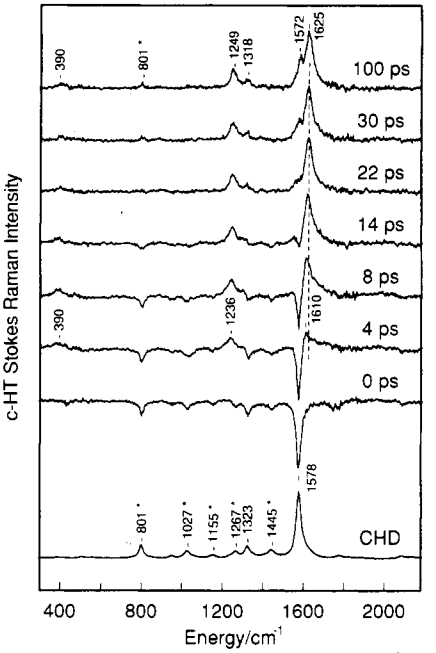

Figure 2. Two-color Stokes resonance Raman difference spectra of the 1,3-cyclohexadiene (CHD)-to-*cis*-hexatriene (c-HT) photoconversion. The probe-only spectrum is given at the bottom of the figure for comparison. Spectra were obtained with 625-μW irradiation in the pump (275 nm) and 180-μW irradiation in the probe (284 nm). The lines at 801, 1027, 1267, and 1445 cm^{-1} are due to the cyclohexane solvent.

To more accurately analyze the appearance kinetics of CHD and c-HT, the difference spectra in Figure 2 were least-squares fit to a linear combination of two basis spectra. The first basis spectrum, representing the c-HT photoproduct, was constructed by adding 2.5% of the probe-only spectrum to the 100-ps difference spectrum to correct for the persistent depletion of CHD and the optical absorbance change. The 100-ps spectrum was chosen since it represents the final spectrum of the photoproduct. The second basis spectrum was the "probe-only" spectrum representing ground-state CHD. The resulting least-squares fit to the difference spectra in Figure 2 is presented as the dashed lines in Figure 3. The overall photoproduct intensity is adequately modeled by the two-component fit, although the exact frequency

(26) Warshel, A.; Karplus, M. *J. Am. Chem. Soc.* **1972**, *94*, 5612–5625.
(27) Myers, A. B.; Mathies, R. A. In *Biological Applications of Raman Spectroscopy: Vol. 2—Resonance Raman Spectra of Polyenes and Aromatics*; Spiro, T. G., Ed.; John Wiley & Sons, Inc: New York, 1987; Vol. 2, pp 1–58.
(28) Xiaopei, C.; Myers, A. B. *J. Chem. Phys.* **1992**, *96*, 6433–6442.
(29) The functional form of the homogeneous broadening was Gaussian for 1,3-cyclohexadiene and Lorentzian for *cis*-hexatriene, in agreement with previous intensity analyses.[15,28,38]

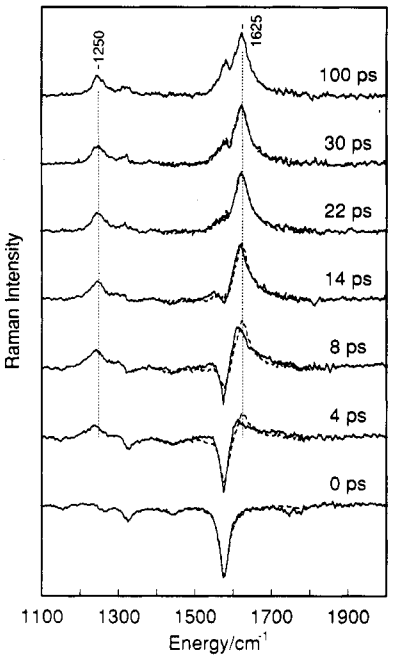

Figure 3. Least-squares analysis of the CHD Stokes difference data. The data are presented as the solid line and the fit to a sum of the CHD and 100-ps c-HT basis spectra is given as the dashed line.

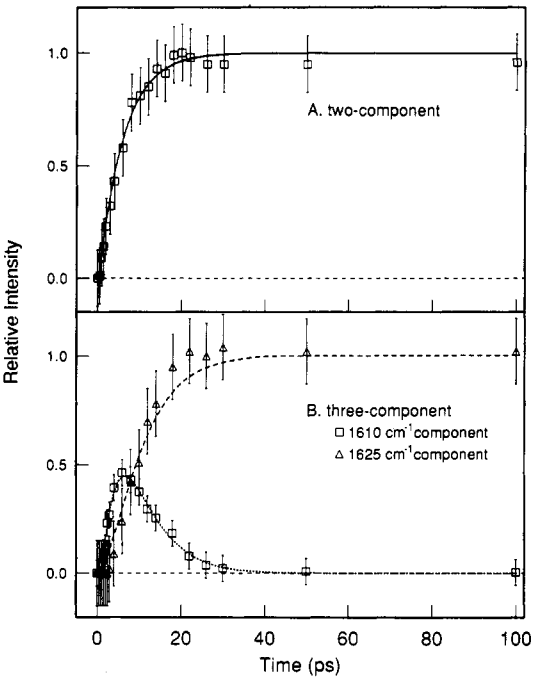

Figure 4. Intensity of the scattering components of *cis*-hexatriene (c-HT) as a function of time after correction for the optical absorption changes. (A) Coefficients of the c-HT scattering component determined from the two-component least-squares fit of the time-resolved Stokes data. The best fit to the data by a single exponential resulted in an appearance time of 6 ± 1 ps. (B) Intensity of the 1610- and 1625-cm^{-1} components determined from the three-component fit to the ethylenic region of the spectrum in Figure 5. The 1610-cm^{-1} component is depicted as □ with best fit to the data resulting in an appearance time of 5 ± 1.5 ps and decay times of 6.5 ● 1.5 (preexponential of 0.87) and 9 ± 2 ps (preexponential of 0.13). The intensity of the 1625-cm^{-1} ethylenic component is presented as △ with the best fit to the data resulting in an appearance time of 7 ± 1.5 ps.

of the early-time photoproduct scattering is not accurately reproduced and suggests that a more detailed analysis is required (see below). Nevertheless, the analysis in Figure 3 will be used to provide an estimate of the CHD ground-state recovery and photoproduct appearance kinetics. After correction for the optical absorbance change, the coefficients for the CHD scattering component indicate that the recovery of CHD is complete within the 1.8-ps time resolution of the experiment. This analysis is complicated by the small extent of depletion and the appearance of photoproduct features which overlap the CHD ethylenic line at 1578 cm^{-1}. The coefficients for the photoproduct component, after correction for the time-dependent optical absorbance change, are presented in Figure 4A. Best fit to a single exponential resulted in an appearance time of 6 ± 1 ps. No significant improvement in the fit was observed by including a second exponential term. The two-component determination of the photoproduct kinetics is in agreement with the initial estimate provided by measurement of the photoproduct ethylenic intensity.

The inability of the two-component fit to model the temporal evolution of the photoproduct vibrational frequencies (Figure 3) indicates that an additional species is present at early times. To determine the time scale and clarify the molecular nature of the c-HT spectral evolution, the photoproduct appearance kinetics were modeled by fitting the ethylenic region of the spectrum to a sum of three components. Three Gaussian peaks with fixed widths and frequencies at 1578, 1610, and 1625 cm^{-1} were employed, and only their amplitudes were allowed to vary. The results of this modeling are presented as the dashed lines in Figure 5. By including an early-time component, the time-dependent frequency shift and amplitude of the photoproduct scattering are adequately reproduced.

The coefficients for the 1610- and 1625-cm^{-1} components were corrected for the time-dependent optical absorbance change and are presented in Figure 4B.[30] The kinetics of the 1610-cm^{-1} species could not be adequately fit assuming double-exponential kinetics, but the inclusion of an additional decay term yielded an excellent fit with a rise time of 5 ± 1.5 ps and decay times of 6.5 ± 1.5 (preexponential factor of 0.87) and 9 ± 2 ps (preexponential factor of 0.13). The 1625-cm^{-1} component was fit assuming a kinetic scheme consistent with its sequential production from the 1610-cm^{-1} component. This analysis resulted in an appearance time of 7 ± 1.5 ps for the 1625-cm^{-1} component.[31] The 1610-cm^{-1} kinetic component could be due to Raman scattering from vibrationally unrelaxed photoproduct which undergoes cooling

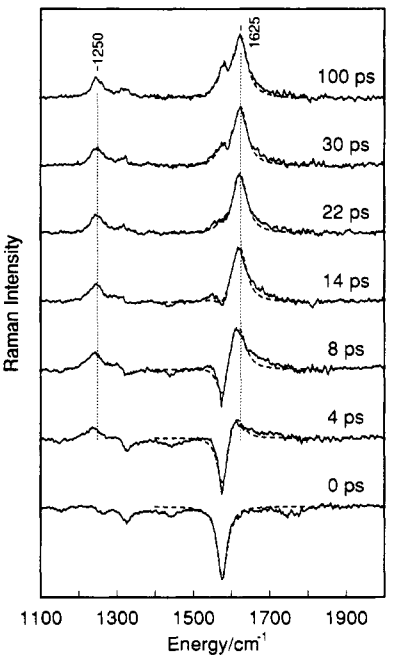

Figure 5. Three-component analysis of the CHD Raman data. Fits were performed with Gaussian peaks at fixed widths of 25 cm^{-1} and frequencies of 1578, 1610, and 1625 cm^{-1}. The fit is presented as the dashed line.

(30) The scattering intensity at 1578 cm^{-1} is due to both ground-state CHD and the c-HT photoproduct; therefore, assignment of this scattering to a unique species is not possible.

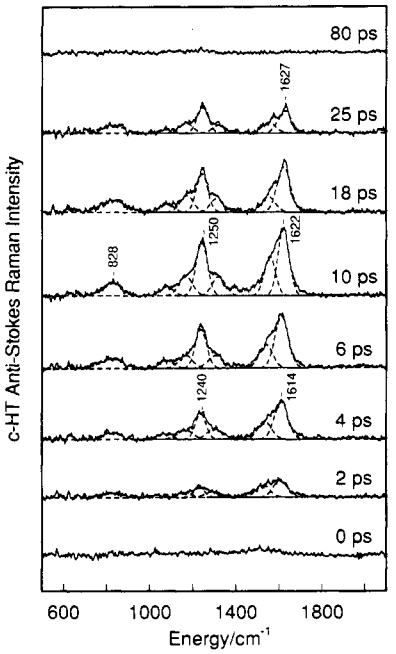

Figure 6. Time-resolved anti-Stokes resonance Raman difference spectra of the photoconversion of 1,3-cyclohexadiene to *cis*-hexatriene. The spectra were obtained with 800-μW irradiation in the pump (284 nm) and 180-μW irradiation in the probe (284 nm). The least-squares fit to the observed anti-Stokes intensity by a sum of Gaussian peaks is presented as the dashed line.

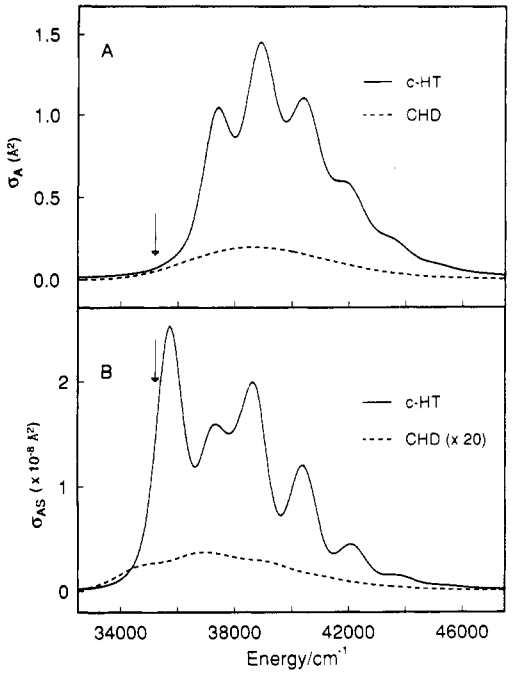

Figure 7. Calculated absorption (A) and anti-Stokes Raman (B) cross sections of c-HT (solid) and CHD (dashed) at 600 K. Calculations were performed utilizing a sum-over-states approach where scattering from initial levels as determined by Boltzmann statistics were explicitly included for all Raman-active modes.[27] Parameters for the calculation (excited-state displacements, transition strength, E_{00}, homogeneous and inhomogeneous broadening) were obtained from previous resonance Raman intensity analyses.[16,28] The anti-Stokes cross section of CHD has been multiplied by 20. The probe wavelength is indicated by the vertical line at 35 211 cm^{-1}.

or conformational relaxation to form the 1625-cm^{-1} species. The spectral evolution observed in the anti-Stokes spectra will allow us to distinguish between these possibilities.

Anti-Stokes Resonance Raman Spectra. To determine the kinetics of vibrational relaxation and to gain insight into the role of molecular cooling in the initial photoproduct dynamics, we obtained time-resolved resonance Raman anti-Stokes spectra of the CHD to c-HT photoconversion. Anti-Stokes difference spectra of the ring-opening of CHD are presented in Figure 6. At 0 ps, very little intensity is evident in the spectrum. By 4 ps, two features at 1614 and 1240 cm^{-1} are observed. The close agreement in frequency between these lines and features observed in the Stokes spectra of the photoproduct indicates that the scattering is due to the ethylenic and single-bond stretch modes of c-HT. The intensity of these two features increases until 10 ps, at which time positive intensity is also observed at 828 cm^{-1}. Furthermore, the frequencies of the photoproduct lines have increased from 1614 and 1240 cm^{-1} to 1622 and 1250 cm^{-1}, respectively. The intensity of these three lines decays between 10 and 80 ps, by which time no anti-Stokes scattering is detected. Further evolution of the ethylenic frequency to 1627 cm^{-1} in the 25-ps spectrum is also observed.

Since the photochemical quantum yield is 0.4, we would expect contributions from both CHD and c-HT to the observed anti-Stokes scattering. To determine the relative contribution of each species to the observed spectra, a sum-over-states calculation utilizing the parameters determined from previous resonance Raman intensity analyses was performed.[16,28] The absorption and anti-Stokes scattering cross sections were calculated at a variety of temperatures ranging from 289 to 800 K with similar results observed at all temperatures. A representative calculation of the absorption spectra at 600 K is presented in Figure 7A, and that for the corresponding ethylenic anti-Stokes cross sections is in 7B. The calculations predict that at our probe frequency, scattering from c-HT will dominate the observed anti-Stokes spectrum. This result is not surprising given that the Raman cross section is dependent on the fourth power of the electronic transition moment, which is 1.63 Å for c-HT and 0.67 Å for CHD (in cyclohexane). Therefore, the intensity observed in the anti-Stokes spectra can be attributed to the c-HT photoproduct only.

The kinetics of c-HT ground-state appearance and vibrational relaxation were determined by fitting the anti-Stokes spectra to a sum of Gaussian peaks. The intensity of the photoproduct ethylenic feature could not be adequately fit assuming a single line, consistent with the observation that this peak has a low-wavenumber shoulder. Therefore, the ethylenic region was least-squares fit by a sum of two Gaussian peaks. The results of the fitting procedure are presented as the dashed lines in Figure 6. Best fit to the ethylenic lines resulted in time-dependent frequency shifts from 1545 to 1560 cm^{-1} and 1614 to 1627 cm^{-1} for the low- and high-frequency components, respectively. The observed intensity could not be fit by constraining the low-frequency component to 1578 cm^{-1}, the frequency of the ethylenic mode of CHD. This is consistent with the predicted dominance of the c-HT anti-Stokes scattering due to its larger anti-Stokes Raman cross section. The changes in intensity versus time of the high- and low-frequency ethylenic components are presented in Figures 8A and B, respectively. Best fit to the data by a double exponential resulted in identical rise times of 8 ± 2 ps and decay times of 9 ± 2 ps.

The kinetics for the lines in the fingerprint region of the anti-Stokes spectrum were also determined by a least-squares analysis. To adequately fit this region, a sum of four peaks centered at 1050, 1150, 1245, and 1318 cm^{-1} was employed. The dominant source of intensity in this region is the single-bond stretch at 1245 cm^{-1}. The intensity of this line as a function of time is presented

(31) The kinetics of the 1610- and 1625-cm^{-1} components were also modeled assuming parallel production of each species from depopulation of the excited state followed by decay of the 1610-cm^{-1} component into the 1625-cm^{-1} species. This analysis resulted in an appearance time of 5 ± 1.5 ps for the 1610-cm^{-1} component with a subsequent decay of 7 ± 1.5 ps. The production of the 1625-cm^{-1} component was dominated by the 7-ps decay of the 1610-cm^{-1} species with direct production from the excited state occurring with a time constant of 76 ± 10 ps. This essentially reduces the parallel scheme to the sequential kinetic model discussed in the text.

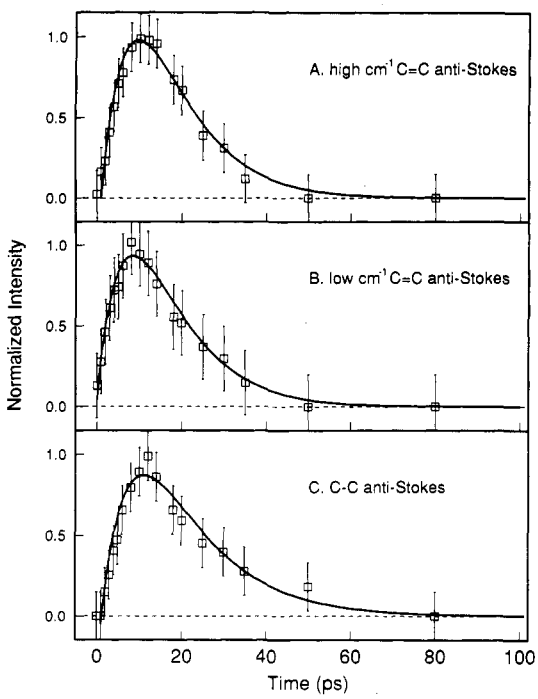

Figure 8. Intensity of the anti-Stokes scattering components of *cis*-hexatriene (c-HT) as a function of time determined from peak fitting. (A) Coefficients of the high-frequency ethylenic component. The best fit to the data by a double exponential resulted in an appearance time of 8 ± 2 ps and a decay time of 9 ± 2 ps. (B) Intensity of the low-frequency ethylenic component. The best fit to the data resulted in an appearance time of 8 ± 2 ps and a decay time of 9 ± 2 ps. (C) Intensity of the c-HT single bond stretch. Best fit to the data resulted in an appearance time of 8 ± 2 ps and a decay time of 14 ± 2 ps.

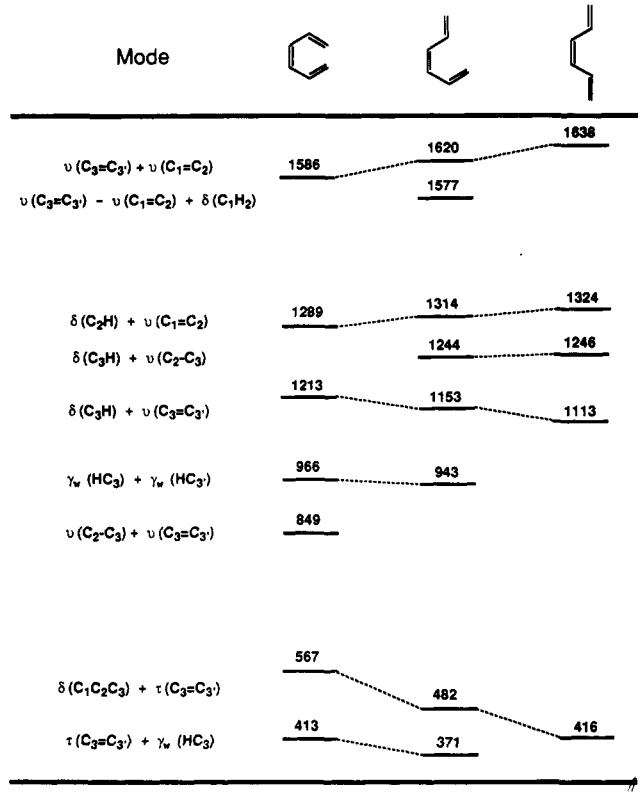

Figure 9. Calculated resonance Raman active modes of the single-bond conformers of *cis*-hexatriene. The approximate character of each mode is given in the left column, with calculated frequencies for each conformer given under the corresponding molecular structure of the conformer. Frequencies are in cm^{-1}, ν = stretch, δ = hydrogen in-plane rocking, γ_w = hydrogen out-of-plane wag, τ = torsion.

in Figure 8C. Best fit by a double exponential resulted in an appearance time of 8 ± 2 ps and a decay time of 14 ± 2 ps. Also, a time-dependent frequency shift of this line from 1236 to 1248 cm^{-1} was observed. The anti-Stokes spectra also exhibit a positive line at 830 cm^{-1}. Although the appearance and decay kinetics of this line were difficult to determine, it is a consistent feature of the data. The appearance and decay of this line combined with the normal mode calculations presented below indicate that the 830-cm^{-1} line is a unique spectroscopic feature of ground-state *all-cis*-hexatriene.

c-HT Vibrational Analysis. To analyze the role of conformational relaxation in the photoproduct spectral evolution, we performed normal mode calculations utilizing the QCFF-π method on the single-bond conformers of c-HT: *di-s-cis*, *mono-s-cis*, and *di-s-trans*.[26] The results of these calculations are summarized in Figure 9. The frequencies and character of the modes determined in this study are in excellent agreement with previous semiempirical and *ab initio* calculations.[32-34] To simplify the presentation of the calculation, we will discuss each region of the spectrum separately.

Ethylenic Region. The *all-cis* conformer is predicted to have the lowest-frequency totally symmetric ethylenic mode. After isomerization of one of the single bonds to form *mono-s-cis*-HT, the in-phase ethylenic line increases in frequency by 30 cm^{-1}. Also, a second out-of-phase ethylenic line at lower frequency is predicted to have intensity consistent with the reduction of symmetry accompanying this conformational relaxation. Isomerization of the other single bond to produce *di-s-trans*-HT leads to a further ~20 cm^{-1} increase in the totally symmetric ethylenic mode, but only a single ethylenic line should be observed, consistent with the Raman spectrum of *di-s-trans*-HT.[28,35-38]

Fingerprint Region. The *mono-s-cis* and *di-s-trans* conformers have modes with mixed single-bond stretch and CH bending character at 1244 and 1246 cm^{-1}, respectively. However, the *all-cis* conformer is not predicted to have a corresponding mode in this region. This can be understood from the geometries of the conformers. Both *mono-s-cis* and *di-s-trans* are close to planar, while the *all-cis* conformer is significantly distorted away from planarity due to steric interaction between the terminal hydrogens resulting in coupling of C–C stretching and H rocking modes. The calculations also predict significant intensity at ~1300 cm^{-1} in all of the conformers due to in-plane hydrogen rocking. The *all-cis* conformer is expected to exhibit intensity at 1213 cm^{-1} corresponding to in-plane rocking of the central hydrogens.

Hydrogen Out-of-Plane (HOOP) Region. The *all-cis* conformer is predicted to have two strong lines in the HOOP region. The first is a HOOP mode about the central double bond at 966 cm^{-1} consistent with the out-of-plane distortion present in this conformer. A similar but less intense mode is also found in *mono-s-cis*-HT, while *di-s-trans*-HT does not demonstrate HOOP intensity consistent with its more planar geometry. The second mode predicted to have intensity solely in the *all-cis* conformer is a mixed C–C stretching and CH_2 rocking mode at 849 cm^{-1}. The presence of Raman intensity in this spectral region is unique to *all-cis*-hexatriene. Consistent with this prediction, the other c-HT conformers do not demonstrate significant intensity in this spectral region.[35-37]

(32) Bock, C. W.; Panchenko, Y. N.; Krasnoshchiokov, S. V.; Pupyshev, V. I. *J. Mol. Struct. (THEOCHEM)* **1986**, *148*, 131–140.
(33) Hemley, R. J.; Brooks, B. R.; Karplus, M. *J. Chem. Phys.* **1986**, *85*, 6550–6564.
(34) Yoshida, H.; Furukawa, Y.; Tasumi, M. *J. Mol. Struct.* **1989**, *194*, 279–299.
(35) Panchenko, Y. N.; Csaszar, P.; Torok, F. *Acta Chim. Hung.* **1983**, *113*, 149–158.
(36) Langkilde, F. W.; Wilbrandt, R.; Nielsen, O. F.; Christensen, D. H.; Nicolaisen, F. M. *Spectrochim. Acta* **1987**, *43A*, 1209–1230.
(37) McDiarmid, R.; Sabljic, A. *J. Phys. Chem.* **1987**, *91*, 276–282.
(38) Amstrup, B.; Langkilde, F. W.; Bajdor, K.; Wilbrandt, R. *J. Phys. Chem.* **1992**, *96*, 4794–4801.

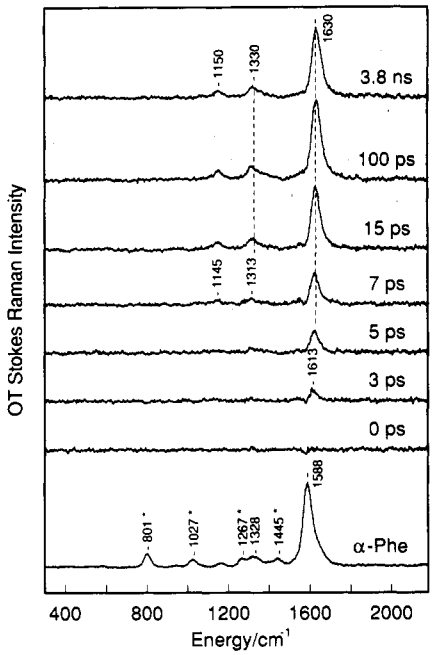

Figure 10. Resonance Raman difference spectra of the photoconversion of α-phellandrene (α-PHE) to 3,7-dimethyl-1,3,5-octatriene.[18] Spectra were obtained with a 275-nm (1.6 mW) pump and a probe at 284 nm (500 μW). A spectrum of α-PHE in cyclohexane obtained at 284 nm is given at the bottom for comparison. Lines due to the cyclohexane solvent are marked with an asterisk.

Low-Frequency Region. Finally, the calculation predicts intensity in modes comprised of skeletal deformations and ethylenic torsions. The *all-cis* conformer is predicted to have a C=C torsional mode at 413 cm^{-1}, while the *mono-s-cis* conformer should have a similar mode at 371 cm^{-1}. A skeletal bending mode is predicted at 567 cm^{-1} for the *all-cis* conformer which shifts down to 416 cm^{-1} in the *di-s-trans* conformer.

α-Phellandrene Raman Kinetics. Two-color, time-resolved Stokes spectra of the photochemical ring-opening of α-phellandrene (α-PHE) to 3,7-dimethyl-1,3,5-octatriene (OT) have been previously reported but are also presented in Figure 10 for comparison with the anti-Stokes data (see below).[18] At 0 ps, a small, negative feature at 1588 cm^{-1} corresponding to the ethylenic line of α-PHE is observed due to ground-state depletion created by the presence of the actinic pulse. At 3 ps, a positive peak at 1613 cm^{-1} is observed and assigned to the OT photoproduct. This feature increases in intensity and shifts up in frequency from 1613 to 1630 cm^{-1} between 3 and 100 ps. At 7 ps, two positive photoproduct peaks are observed at 1313 and 1145 cm^{-1}. These lines gain intensity and shift up to 1320 and 1150 cm^{-1}, respectively, by 100 ps. No further evolution in the spectrum is observed between 100 ps and 3.8 ns. A plot of the photoproduct ethylenic intensity versus time, corrected for the change in optical absorbance, is presented in Figure 11A. The best fit to a single exponential resulted in an appearance time of 11 ± 2 ps for the OT photoproduct. No significant improvement in fit was observed by including a second exponential term.

Anti-Stokes Raman difference spectra of the photoconversion of α-PHE to OT are presented in Figure 12. A single, strong feature at 1608 cm^{-1} is observed at 2 ps and is assigned as the ethylenic stretch of the OT photoproduct. This line increases in intensity between 0 and 10 ps, by which time features at 1318 and 1145 cm^{-1} are also observed. The correspondence between these frequencies and those observed in the OT Stokes spectrum indicates that these lines are also due to the appearance of photoproduct. In the 25-ps spectrum, the frequency of the photoproduct ethylenic line has shifted up to 1630 cm^{-1}, identical to the observed frequency in the 100-ps Stokes spectrum of OT. The anti-Stokes scattering decreases in intensity between 10 and 40 ps. The intensity of the photoproduct anti-Stokes ethylenic line is plotted as a function of time in Figure 11B. Best fit to the data by a double exponential resulted in an appearance time of 8 ± 2 ps and a decay time of 9 ± 2 ps.

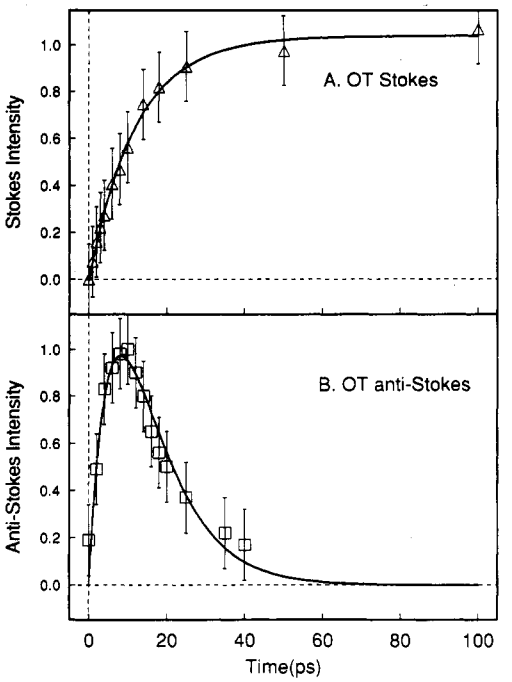

Figure 11. (A) Stokes intensity of the ethylenic stretch of OT versus time after correction for the optical absorption changes.[18] The best fit to the data by a single exponential resulted in an appearance time of 11 ± 2 ps. (B) Anti-Stokes intensity of the ethylenic stretch of 3,7-dimethyl-1,3,5-octatriene as a function of time. The best fit to the data by a double exponential resulted in an appearance time of 8 ± 2 ps and a decay time of 9 ± 2 ps.

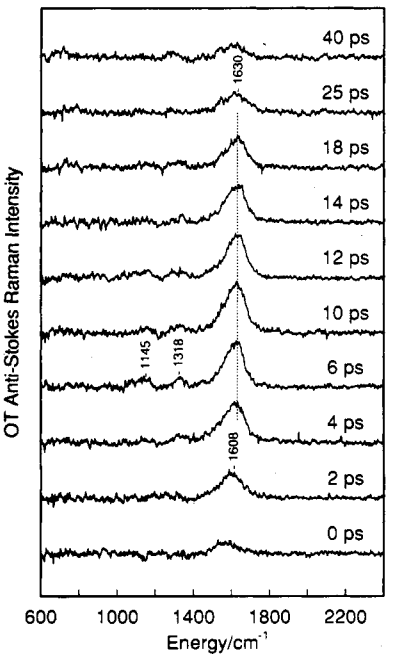

Figure 12. Anti-Stokes resonance Raman difference spectra of the photoconversion of α-phellandrene to 3,7-dimethyl-1,3,5-octatriene. The spectra were obtained with 800-μW irradiation in the pump (284 nm) and 180-μW irradiation in the probe (284 nm).

Discussion

CHD Photoproduct Appearance, Vibrational, and Conformational Relaxation Kinetics. The two-component fit to the time-resolved Stokes data (Figure 4A) demonstrates that ground-state *cis*-hexatriene (c-HT) photoproduct appears with a time constant

of 6 ps after photolysis of CHD. This is consistent with our earlier one-color results.[17] Although this analysis is adequate, the inability of the two-component fit to reproduce the time-dependent increase in photoproduct ethylenic frequency observed in the Stokes spectra demonstrates that additional intermediate ground-state species are present. To fully understand the dynamics of photoproduct formation, we must determine the origin of the c-HT spectral evolution in both the Stokes and anti-Stokes data.

One interpretation of the time-dependent increase in photoproduct ethylenic frequency from 1610 to 1625 cm^{-1} is that this shift is due to intermolecular vibrational relaxation, resulting in the depopulation of higher levels of an anharmonic ground-state potential surface. Recent experiments on 1,3,5-cycloheptatriene attributed a 7-cm^{-1} ethylenic frequency increase in the Stokes spectrum to the presence of vibrationally unrelaxed molecules on the ground-state surface.[20] However, experiments on other electrocyclic ring-opening reactions have demonstrated larger $\sim$25 cm^{-1} evolution in the photoproduct ethylenic frequency, while the anharmonicity constant for ethylenic modes of polyenes is expected to be only $\sim$2 cm^{-1}.[18,39,40] Given the limited population of vibrational levels greater than ν_2 (see below), the observed frequency evolution is much larger than that expected for shifts due exclusively to thermal relaxation.

A second possibility is that the frequency evolution is due to coupling between the observed ethylenic modes and low-frequency modes undergoing resonant energy exchange with the solvent.[41,42] In this "exchange theory", evolution in both vibrational frequencies and line widths is predicted. However, the c-HT Stokes and anti-Stokes intensities could be adequately modeled with Gaussian peaks having fixed widths. The absence of photoproduct line width evolution as well as the magnitude of the frequency shift and modest anharmonicity along skeletal stretching coordinates indicates that the observed spectral evolution is not due to coupling between the Franck–Condon active coordinates and low-frequency modes.

Conformational relaxation of the c-HT photoproduct on the ground-state surface is the best explanation for the observed spectral evolution. The vibrational spectra presented here provide clear evidence for the presence of *all-cis*-HT and *mono-s-cis*-HT. In the anti-Stokes spectra (Figure 8 at 10 ps), an intense line at 829 cm^{-1} as well as intensity at 1050 cm^{-1} is observed, in agreement only with the predicted CH_2 rocking and HOOP modes of *all-cis*-HT. *The presence of scattering at 829 cm^{-1} strongly argues for the presence of the all-cis conformer on the ground-state surface.* Also, the anti-Stokes scattering at 829 cm^{-1} and the absence of corresponding intensity in the Stokes spectra indicate that this scattering corresponds to a structural precursor of the long-time photoproduct. Finally, the evolution in the photoproduct ethylenic frequency and the presence of two ethylenic lines in the 100-ps Stokes spectrum is consistent with conformational relaxation of *all-s-cis*-HT to *mono-s-cis*-HT on the ground-state surface. Therefore, we are directly observing the isomerization of *all-cis*-hexatriene to form the *mono-s-cis* conformer.

The three-component analysis of the Stokes data allows for the deconvolution of the individual c-HT conformer kinetics. The 1610-cm^{-1} component has an appearance time of 5 ps and biexponential decay with a principle component of 6.5 ps and a minor channel decaying in 9 ps. The 1625-cm^{-1} component appears with a time-constant of 7 ps, with its appearance delayed relative to the 1610 cm^{-1} line. The inability of a kinetic scheme on the basis of parallel production of each species followed by vibrational relaxation of the 1610-cm^{-1} form to the 1625-cm^{-1} species to model the observed kinetics demonstrates that the 1610-cm^{-1} component must be a structural precursor of the 1625-cm^{-1} species.[31] Since the increase in ethylenic frequency is consistent with conformational relaxation (Figure 9), we conclude that the scattering at 1610 cm^{-1} is due to *all-cis*-HT and that the intensity at 1625 cm^{-1} corresponds to *mono-s-cis*-HT produced from relaxation of the initial ground-state conformer. The relative amplitude of the 7-ps decay component for 1610 cm^{-1} (*all-cis*-HT) Stokes intensity also demonstrates that conformational relaxation dominates the observed spectral evolution. The agreement between the smaller decay component and the 9-ps vibrational relaxation time determined from the decay of the photoproduct anti-Stokes intensity indicates that the contribution of vibrational relaxation to the observed spectral evolution is small, consistent with the above discussion.

The barrier for ground-state, single-bond isomerizations is known to be $\sim$4.2 kcal/mol; therefore, a 7-ps isomerization time is much faster than expected.[43,44] This rate is probably enhanced by the steric repulsion of the terminal hydrogens in *all-cis*-HT which raises the ground-state enthalpy of this conformer as well as the increase in molecular temperature due to incomplete vibrational cooling on this time scale.[45] Although further relaxation to *di-s-trans*-HT cannot be ruled out, the majority of the features observed in the Raman spectra can only be explained by the presence of *all-cis* and *mono-s-cis*-HT on the ground-state surface.

Determination of the Molecular Temperature of *cis*-Hexatriene. The ethylenic and single-bond anti-Stokes lines of c-HT exhibit different kinetics: the single-bond stretch decays in 14 $\pm$ 2 ps, while the ethylenic line decays in 9 $\pm$ 2 ps. This variance probably reflects an increase in population of higher levels of the ground-state vibrational manifold for the lower frequency single-bond mode relative to the higher frequency ethylenic rather than mode-specific vibrational relaxation. The intensity in the anti-Stokes spectrum for a given mode can be expressed as

$$I = \sum_{i=1}^{n} \sigma_i P_i L$$

where σ_i is the anti-Stokes cross section for vibrational level i, P_i is the level population, and L is the laser power. The summation is carried out over the total number of vibrational levels along the normal coordinate being considered. In order to evaluate this expression, we must first estimate the population in each level of the ground-state vibrational manifold of a normal coordinate at a given temperature. Assuming (1) that no energy loss occurs in the excited state, (2) that the excess energy of the molecule is deposited into vibrational degrees of freedom, and (3) that the excess energy is partitioned between all modes equally as a result of complete intramolecular vibrational energy relaxation, we estimate a molecular temperature of 2100 K. With this temperature, the Boltzmann populations in the first three vibrational levels along the ethylenic coordinate would be ν_0 = 0.67, ν_1 = 0.22, and ν_2 = 0.07. Also, the populations along the single-bond coordinate would be ν_0 = 0.58, ν_1 = 0.24 and ν_2 = 0.10. Even at this elevated temperature, the majority of population is located in the lowest three vibrational levels of either coordinate. If we consider the anti-Stokes cross section for each vibrational level, the cross section for the ν = 0 level is 0. To estimate the relative anti-Stokes cross sections, we applied the sum-over-states calculation to the ν = 1 and ν = 2 vibrational levels. For the ethylenic coordinate, $\sigma_{\nu=1}$ is twice as large as $\sigma_{\nu=2}$, while these two levels have equal cross sections for the single-bond stretch at our probe wavelength. Given these relative populations and

(39) Kohler, B. E.; Spangler, C.; Westerfield, C. *J. Chem. Phys.* **1988**, *89*, 5422–5428.
(40) In our experiments on the photochemical ring-opening of 1,3,5-cyclooctatriene, a 25-cm^{-1} increase in the photoproduct ethylenic frequency was observed, while the anharmonicity for the corresponding mode in *all-trans*-octatetraene is 2 cm^{-1}.[17,39]
(41) Shelby, R. M.; Harris, C. B.; Cornelius, P. A. *J. Chem. Phys.* **1979**, *70*, 34–41.
(42) Harris, C. B.; Shelby, R. M.; Cornelius, P. A. *Chem. Phys. Lett.* **1978**, *57*, 8–14.
(43) Carreria, L. A. *J. Chem. Phys.* **1975**, *62*, 3851–3854.
(44) Ackerman, J. R.; Kohler, B. E. *J. Chem. Phys.* **1984**, *80*, 45–50.
(45) Allinger, N. L.; Tai, J. C. *J. Am. Chem. Soc.* **1977**, *99*, 4256–4259.

cross sections, and observed anti-Stokes scattering can roughly be considered to originate from $v = 1$ only.[46-49] In this limit, the ratio of ethylenic to single-bond stretch anti-Stokes scattering reduces to

$$\frac{I_{C=C}}{I_{C-C}} = \frac{\sigma_{C=C}}{\sigma_{C-C}} \exp\left(\frac{-\Delta E}{kT}\right)$$

where ΔE corresponds to the difference between the ethylenic and single-bond stretch energies (374 cm^{-1}), k is Boltzmann's constant, and T is the temperature. Since the anti-Stokes cross sections correspond to the $v = 1$ level for both lines, this ratio is a constant. Therefore, as the molecular temperature decreases, the ratio of ethylenic to single-bond anti-Stokes intensity will decrease as well. The more rapid decay of the 1624-cm^{-1} anti-Stokes intensity relative to the single-bond intensity at 1250 cm^{-1} is consistent with molecular cooling in the limit of Boltzmann statistics.

We can utilize this relationship between the ethylenic and single-bond anti-Stokes intensities to estimate the molecular temperature of c-HT as a function of time. Hopkins and co-workers have developed a similar formalism to determine the molecular temperature of the porphyrin ring in deoxyhemoglobin after photoexcitation.[46,47] Their approach applied to our experiment can be expressed by the following equation:

$$\frac{I_{C=C}(T_2)/I_{C=C}(T_1)}{I_{C-C}(T_2)/I_{C-C}(T_1)} = \exp\left(\frac{-\Delta E}{k} \times \left(\frac{1}{T_2} - \frac{1}{T_1}\right)\right)$$

The need to know the absolute resonance Raman anti-Stokes cross sections is eliminated by comparing the ethylenic and single-bond intensities at a given temperature (T_2) to those at a reference temperature (T_1). Since the observed anti-Stokes scattering is dominated by the c-HT photoproduct, there is no observed intensity in the low-photolysis, probe-only spectrum, prohibiting a determination of the anti-Stokes intensities at room temperature. However, we can use the 35-ps spectrum as our reference by comparing the photoproduct Stokes and anti-Stokes intensities at this delay time following the formalism developed by Champion and co-workers.[48,49] At this time point, the ratio of Stokes to anti-Stokes scattering for the high-frequency ethylenic line (1624 cm^{-1}) is 0.028 ± 0.01. With this ratio, the E_{00} of c-HT (37 300 cm^{-1}), and the probe wavelength (35 211 cm^{-1}), we calculate that the molecular temperature is 350 ± 30 K. An elevated equilibrium temperature relative to that of the bulk solvent is supported by studies on azulene where energy exchange between the molecule and the neighboring solvent shell occurs in ~20 ps with heat flow to the remaining solvent taking place at longer times.[50-52] Using this value as our reference temperature, we have calculated the temperature of the photoproduct determined by the ethylenic and single-bond anti-Stokes intensities at various delay times relative to the 35-ps spectrum (Figure 13). At 4 ps, the temperature of the c-HT photoproduct is 1500 ± 500 K. We can determine the initial molecular temperature by fitting the time-dependent molecular temperature to the following simple decay:[53]

$$T(t) - T_{eq} = (T_m - T_{eq}) \times e^{-t/\tau_v}$$

where T_{eq} is the equilibrium temperature of the molecule and T_m is the molecular temperature at zero time. For simplicity, we assume that intramolecular vibrational equilibration is instantaneous, allowing for a statistical temperature at zero time. We define T_{eq} as the temperature at 35 ps. Best fit to the temperature evolution resulted in a temperature relaxation time of ~15 ps with an initial molecular temperature of 1900 K. This large initial temperature suggests that little energy is lost during the excited-state evolution and subsequent coupling to the ground state. In contrast, 65% of the excess energy is lost to the environment during the course of the isomerization of *cis*-stilbene.[53] The rapid intermolecular energy loss in stilbene is thought to involve friction with the solvent due to the large displacement accompanying isomerization. The magnitude of geometric evolution is expected to be more limited for the ring-opening reactions presented here.

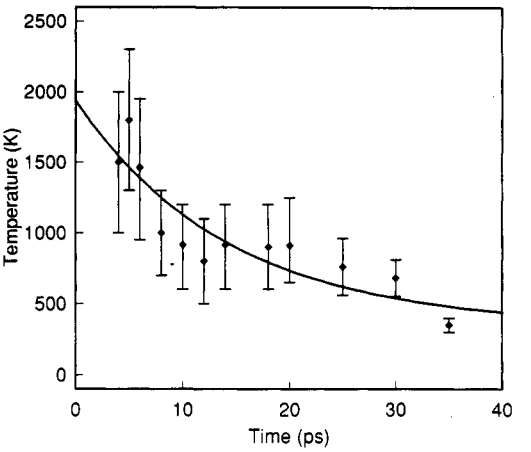

Figure 13. Calculated temperature of the *cis*-hexatriene (c-HT) photoproduct as a function of delay time. Temperatures were determined by considering the ratio of the anti-Stokes intensities of the ethylenic and single-bond stretches to intensities observed in the 35-ps spectrum. The 35-ps spectrum was determined to represent c-HT at 350 ± 30 K as explained in the text. The solid line is the fit to the molecular temperature assuming an exponential decay. Best fit to the data resulted in a temperature decay time of 15 ± 10 ps from an initial molecular temperature of 1900 K.

The small extent of energy loss in the excited state of CHD is consistent with placement of the lower-lying $2A_1$-state origin ~5000 cm^{-1} below the initially prepared $1B_2$ state as well as calculations on the conversion of CHD to c-HT, where the energy difference between the minima of these surfaces is predicted to be modest.[54-56] Given the origin of the $2A_1$ state determined by Kohler and co-workers and assuming that the excess vibrational energy created by decay of the $1B_2$ surface is lost to the solvent, we estimate an initial photoproduct temperature of ~1950 K. If we also assume that the 6-ps appearance time represents internal conversion from the $2A_1$ surface and that the rate of intermolecular vibrational cooling in this state is similar to that in the ground state, the estimated 1900 ± 500 K initial temperature corresponds to an $2A_1$-state origin which is 30 000 ± 9000 cm^{-1} higher in energy than the ground state and ~5000 cm^{-1} lower than the $1B_2$-state origin.

The Photochemistry of α-PHE. The Stokes and anti-Stokes spectra of α-PHE presented here demonstrate that the observed kinetics and ground-state dynamics for c-HT are not unique to CHD photochemistry but are a general feature of electrocyclic ring-opening reactions. 3,7-Dimethyl-1,3,5-octatriene (OT) produced from the photolysis of α-PHE appears on the ground state

(46) Hopkins, J. B.; Xu, X.; Lingle, R.; Zhu, H.; Yu, S.-C. *Biomolecular Spectroscopy II*; SPIE: Los Angeles, 1991; pp 221–226.
(47) Lingle, R.; Xu, X.; Zhu, H.; Yu, S.-C.; Hopkins, J. B. *J. Am. Chem. Soc.* **1991**, *113*, 3992–3994.
(48) Schomacker, K. T.; Bangcharoenpaurpong, O.; Champion, P. M. *J. Chem. Phys.* **1984**, *80*, 4701–4717.
(49) Schomacker, K. T.; Champion, P. M. *J. Chem. Phys.* **1989**, *90*, 5982–5993.
(50) Sukowski, U.; Seilmeier, A.; Elasesser, T.; Fischer, S. F. *J. Chem. Phys.* **1990**, *93*, 4094–4101.
(51) Wild, W.; Seilmeier, A.; Gottfried, N. H.; Kaiser, W. *Chem. Phys. Lett.* **1985**, *119*, 259–263.
(52) Scherer, P. O. J.; Seilmeier, A.; Kaiser, W. *J. Chem. Phys.* **1985**, *83*, 3948–3957.
(53) Sension, R. J.; Repinec, S. T.; Hochstrasser, R. M. *J. Chem. Phys.* **1990**, *93*, 9185–9188.
(54) Buma, J. W.; Kohler, B. E.; Song, K. *J. Chem. Phys.* **1990**, *92*, 4622–4623.
(55) Buma, J. W.; Kohler, B. E.; Song, K. *J. Chem. Phys.* **1991**, *94*, 4691–4698.
(56) Share, P. E.; Kompa, K. L.; Peyerimhoff, S. D.; van Hermet, M. C. *Chem. Phys.* **1988**, *120*, 411–419.

in ~10 ps, similar to the 6-ps appearance time of c-HT. Furthermore, the 9-ps vibrational cooling time of the α-PHE product is also identical to the relaxation time observed in c-HT. Although the slight difference in appearance kinetics may indicate that the production of ground-state photoproduct is slowed by the presence of the bulky isopropyl group, the lack of a dramatic change in kinetics demonstrates that the presence of alkyl substituents on the CHD ring does not dramatically affect the rate of internal conversion to the ground-state surface or the rate of vibrational relaxation. However, the presence of alkyl substituents may affect the initial excited-state dynamics. The increase in the OT anti-Stokes ethylenic frequency from 1608 to 1630 cm^{-1} is similar to the 17-cm^{-1} increase in frequency observed in the Stokes data as well as the evolution observed in CHD. This similarity suggests that OT also undergoes conformational relaxation from *all-s-cis* to the *mono-s-cis* species on the ground-state surface.

Summary

The data and analysis presented here allow us to form a more complete picture of the dynamics of pericyclic photochemical ring-opening reactions. A schematic reaction coordinate for the ring-opening of CHD is presented in Figure 14. After excitation, CHD propagates along the predicted conrotatory reaction coordinate undergoing rapid, nonradiative decay to the lower $2A_1$ surface similar to the behavior observed in longer polyenes.[12,57] The vibrationally hot *all-cis*-HT ground-state photoproduct is then produced in 6 ps. Although the barrier to single- and double-bond isomerizations on the $2A_1$ surface are relatively small for linear polyenes,[58,59] the presence of ground-state *all-cis*-HT demonstratesthat neither process is involved in internal conversion from the $2A_1$ state. Once the ground-state is populated, vibrational cooling occurs in 9 ps along with the 7-ps conformational relaxation of *all-cis*-HT to *mono-s-cis*-HT. ***This study represents the first determination of the photoproduct formation and vibrational relaxation dynamics in electrocyclic ring-opening reactions.***

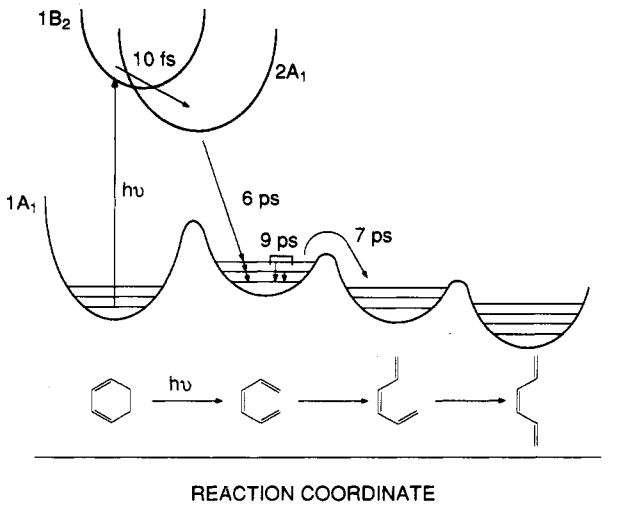

Figure 14. Schematic reaction coordinate for the photochemical ring-opening of 1,3-cyclohexadiene.

Acknowledgment. The authors would like to thank Andy Shreve for his development of the calculation used to determine the anti-Stokes cross sections. This work was supported by a grant from the NSF (CHE 91-20254).

(57) Hudson, B.; Kohler, B. *Annu. Rev. Phys. Chem.* **1974**, *25*, 437–460.
(58) Ackerman, J. R.; Kohler, B. E.; Huppert, D.; Rentzepis, P. M. *J. Chem. Phys.* **1982**, *77*, 3967–3973.
(59) Ackerman, J. R.; Kohler, B. E. *J. Am. Chem. Soc.* **1984**, *106*, 3681–3682.